Electronic Supplementary Material (ESI) for Journal of Materials Chemistry A

Journal of Materials Chemistry A

Supplementary Information for:

Dichotomous adsorption behaviour of dyes on an amino-functionalised metal-organic framework, amino-MIL-101(Al)

Enamul Haque, Victor Lo, Andrew I. Minett, Andrew T. Harris and Tamara L. Church*
Laboratory of Sustainable Technology, School of Chemical & Biomolecular Engineering,
The University of Sydney, NSW 2006, Australia.
E-mail: tamara.church@sydney.edu.au

Contents **Page**

1. Dyes: Structures and Calibration Curves

The structures of methylene blue (MB) and methyl orange (MO) are shown in Figure S1, and UV-vis calibration curves for the dyes are presented in Figure S2.

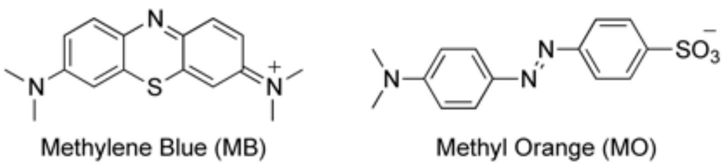

Fig. S1. Structures of the methylene blue and methyl orange dyes.

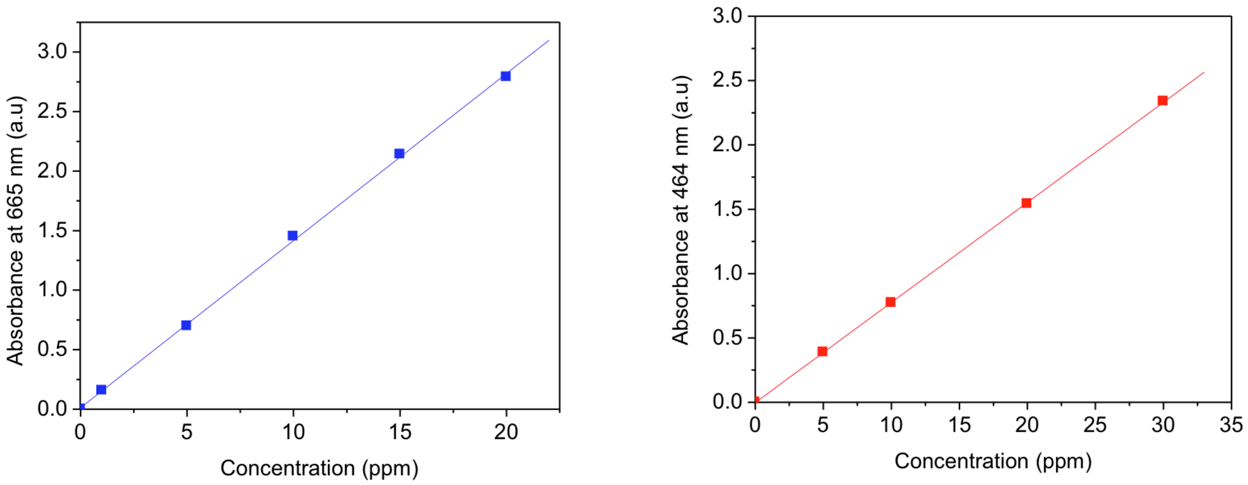

Fig. S2. UV-vis calibration curves for MB (left) and MO (right).

Electronic Supplementary Material (ESI) for Journal of Materials Chemistry A

2. Characterisation of amino-MIL-101(Al)

Amino-MIL-101(Al) was characterised by X-ray diffraction (XRD), N_2 adsorption-desorption, and thermogravimetry, as shown in Figures S3−S5. X-ray photoelectron spectroscopy (XPS) data for amino-MIL-101(Al) is discussed and shown on page S9.

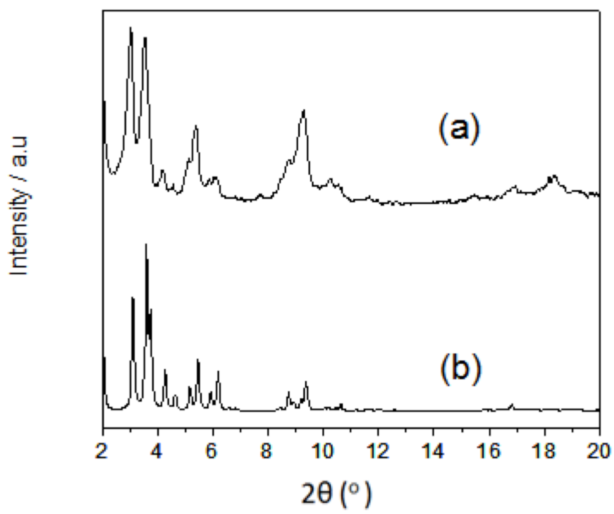

Fig. S3. (a) Experimental XRD pattern of amino-MIL-101(Al); (b) Simulated pattern of MIL-101 phase.

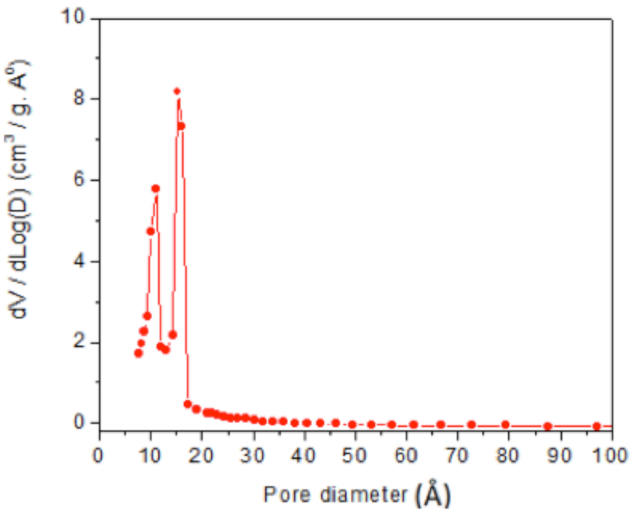

Fig. S4. Pore size distribution curve of amino-MIL-101(Al). Calculated from the adsorption branch of the N_2 adsorption-desorption isotherm (acquired at −196 °C) using BJH method.

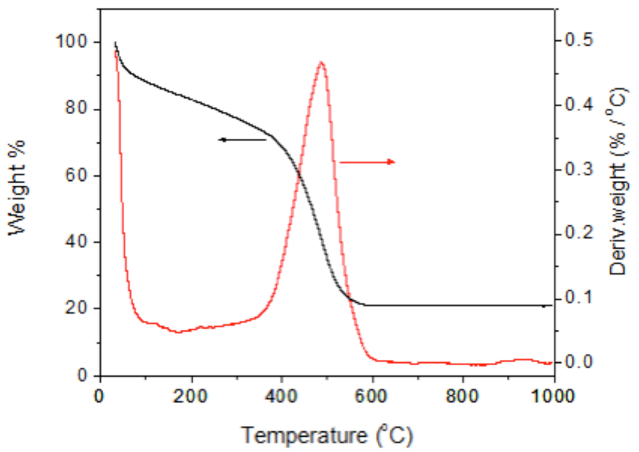

Fig. S5. Thermogravimetric analysis of amino-MIL-101(Al) under air flow of 60 mL min^{-1} at a heating rate of 5 °C min^{-1}.

3. Adsorption of methylene blue (MB)

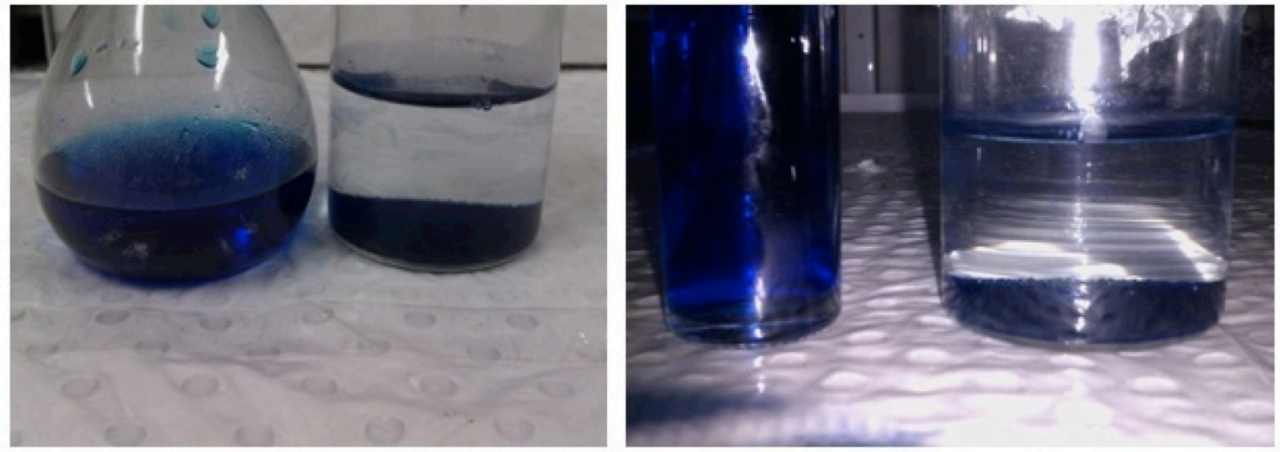

Fig. S6. Digital images of before and after adsorption of MB by amino-MIL-101(Al). $[MB]_0$ = 50 ppm, *t* = 6 h, $m_{amino\text{-}MIL\text{-}101(Al)}$ = 0.01 g.

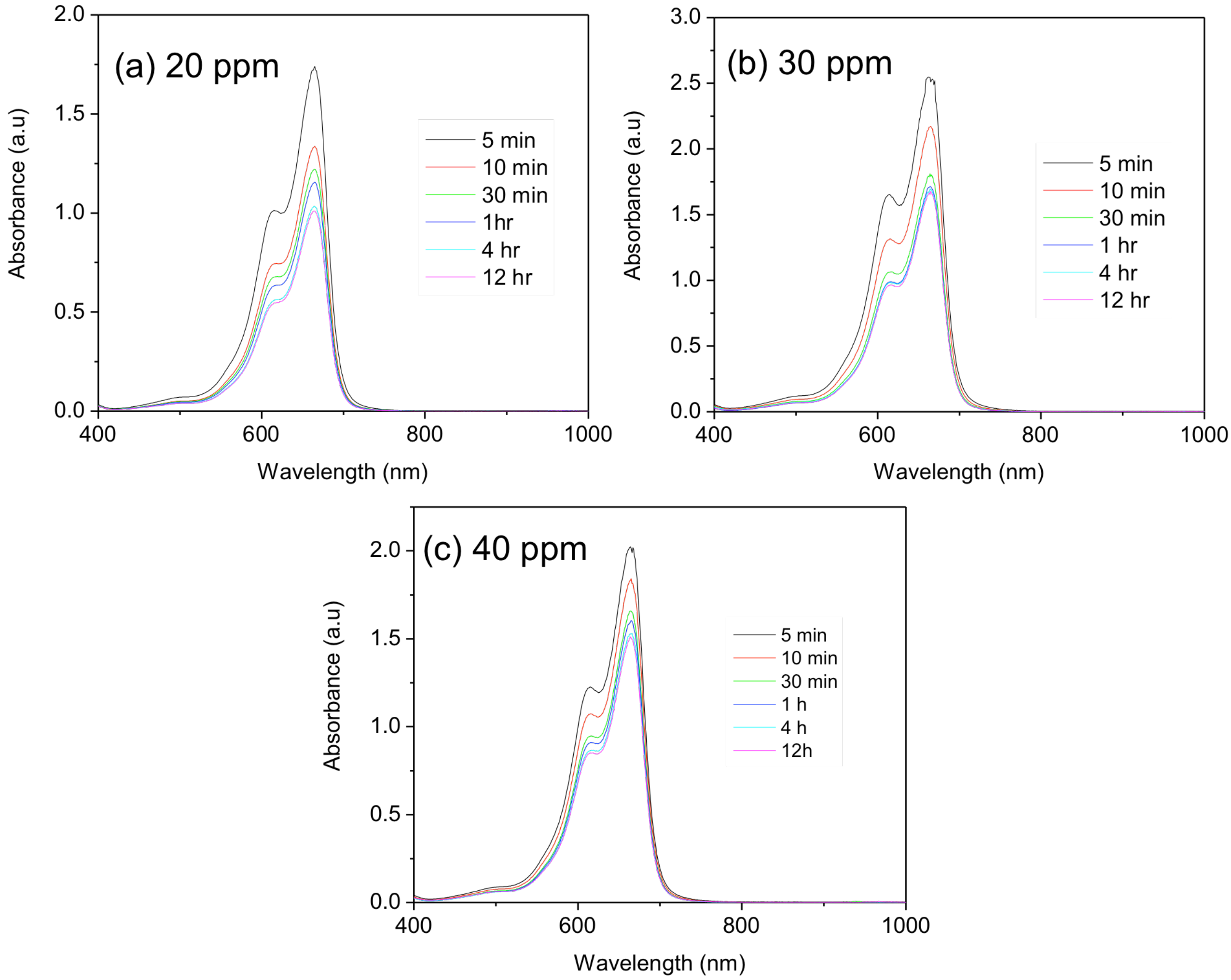

Fig. S7. UV-visible spectra of MB solutions after exposure to 5 mg of amino-MIL-101(Al) at 30 °C. (a) $[MB]_0$ = 20 ppm, (b) $[MB]_0$ = 30 ppm, (c) $[MB]_0$ = 40 ppm.

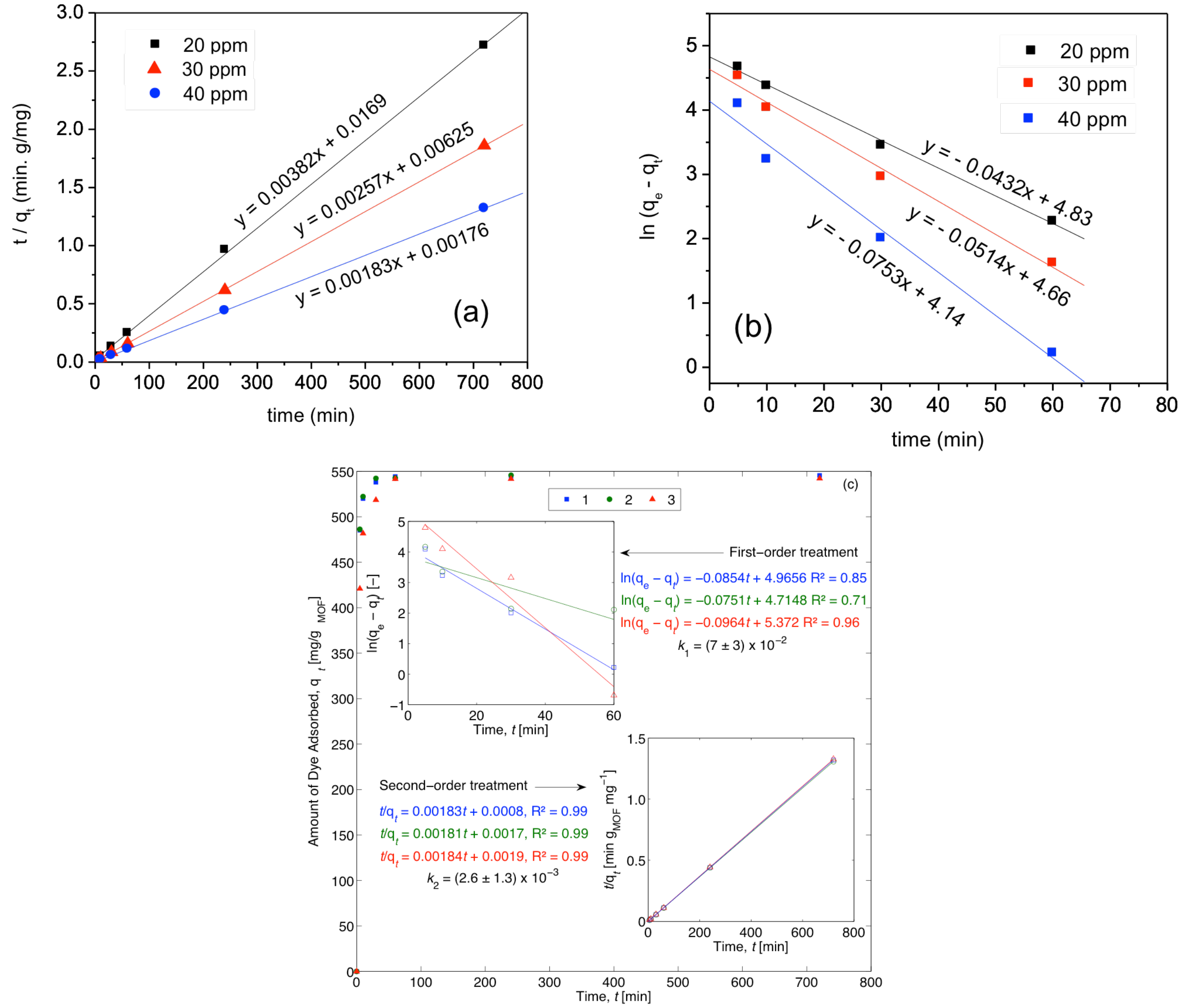

Fig. S8. Plots of (a) pseudo-second-order and (b) pseudo-first-order kinetics for MB adsorption over 5 mg amino-MIL-101(Al) at 30 °C and $[MB]_0$ = 20, 30 or 40 ppm. (c) Three replicates of the adsorption of MB over 5 mg amino-MIL-101(Al) at 30 °C and $[MB]_0$ = 40 ppm, with accompanying kinetic fits.

The maximum adsorption capacity of amino-MIL-101(Al) for MB compared favourably to those of many reported sorbents. A comparison is given in Table S1.

Table S1. Maximum adsorption capacities of methylene blue (MB) on various adsorbents.

Adsorbent	Maximum Adsorption Capacity, Q_o (mg g^{-1})	Reference
Chitosan-*g*-poly(acrylic acid)–vermiculite hydrogel composite	1685	*J. Environ. Sci.* **2010**, *22*, 486–493.
Teak wood bark	915	*Water Air Soil Pollut.* **1999**, *114*, 423–438.
Poly(methacrylic acid)-modified biomass of baker's yeast	870	*J. Hazard. Mater.* **2009**, *168*, 1147–1154.
Amino-MIL-101-Al	**762 ± 12**	**This work**
Poly(amic acid)-modified biomass of baker's yeast	680	*Appl. Biochem. Biotechnol.* **2010**, *160*, 1394–1406.
Magnetic modified beer yeast	609	*Environ. Sci. Pollut. Res.* **2013**, *20*, 543–51.

Activated carbon produced from New Zealand coal	588	*Chem. Eng. J.* **2008**, *135*, 174–184.
Papaya seed	556	*J. Hazard. Mater.* **2009**, *162*, 939–944.
Activated carbon derived from periwinkle	500	*Chem. Ecol.* **2008**, *24*, 285–295.
Poly(vinylidene fluoride)-derived activated carbon fibers	486	*Carbon* **2001**, *39*, 207–214.
Filtrasorb 400	476	*Chem. Eng. J.* **2008**, *135*, 174–184.
Straw activated carbon	472	*Dyes Pigm.* **2001**, *51*, 25–40.
Grass waste	458	*J. Hazard. Mater.* **2009**, *166*, 233–238.
Bamboo-based activated carbon	454	*J. Hazard. Mater.* **2007**, *141*, 819–825.
Coal-based activated carbon from anthracite	448	*Ind. Eng. Chem. Res.* **1991**, *30*, 2411–2416.
Activated carbon (molasses/sulphuric acid)	435	*J. Hazard. Mater.* **2005**, *118*, 259–263.
Activated carbon prepared from coconut husk	435	*J. Hazard. Mater.* **2008**, *154*, 337–346.
Jute fiber carbon	226	*J. Colloid Interface Sci.* **2005**, *284*, 78–82.
Vetiver roots activated carbon	423	*J. Hazard. Mater.* **2009**, *165*, 1029–1039.
Caulerpa lentillifera	417	*Bioresour. Technol.* **2007**, *98*, 1567–1572.
Olive-waste-derived activated carbon	403	*Environ. Technol.* **1998**, *19*, 1203-1212.
Activated carbon	400	*J. Hazard. Mater.* **2006**, *134*, 237–244.
Mesoporous carbons prepared using alkaline-treated zeolite	380	*Colloids Surf. A* **2009**, *333*, 115–119.
Activated carbon from Venezuelan bituminous coal	380	*Chem. Eng. J.* **2008**, *135*, 174–184.
Carbons prepared from coffee grounds	370	*J. Hazard. Mater.* **2010**, *175*, 779–788.
Rice husk activated carbon	344	*Dyes Pigm.* **2001**, *51*, 25–40.
Peat	324	*J. Hazard. Mater.* **2007**, *144*, 412–419.
Coal	327	*Water Air Soil Pollut.* **1999**, *114*, 423–438.
Black cherry stones	322	*J. Hazard. Mater.* **2010**, *180*, 656–661.
Rice husk	313	*Water Air Soil Pollut.* **1999**, *114*, 423–438.
Clay	300	*Ann. Chim.* **2000**, *25*, 615–626.
Spent tea leaves	300	*J. Hazard. Mater.* **2009**, *161*, 753–759.
Filtrasorb 400	299	*J. Hazard. Mater.* **2009**, *165*, 291–299.
Guava (*Psidium guajava*) leaf	295	*J. Hazard. Mater.* **2008**, *152* , 276–286.
Activated carbon prepared from rattan sawdust	294	*Dyes Pigm.* **2007**, *75*, 143–149.
Montmorillonite clay	289	*J. Colloid Interface Sci.* **2009**, *332*, 46–53.
Jackfruit peel	286	*J. Hazard. Mater.* **2009**, *162*, 344–350.
Oregano stem	286	*Energy Fuels* **2002**, *20*, 2636–2641.
Alga *Sargassum muticum* seaweed	279	*J. Chem. Technol. Biotechnol.* **2005**, *80*, 291–298.
Coconut-shell-derived activated carbon	278	*Dyes Pigm.* **2001**, *51*, 25–40.
Cotton waste	278	*Water Air Soil Pollut.* **1999**, *114*, 423–438.
Activated sludge biomass	256	*J. Hazard. Mater.* **2004**, *108*, 183–188.
Jute fiber carbon	226	*Chemosphere* **2001**, *45*, 51–58.
Diatomite	198	*J. Environ. Manage.* **2003**, *69*, 229–238.
MOF-235	187	*J. Hazard. Mater.* **2011**, *185*, 507–511.
Bentonite	175	*J. Hazard. Mater.* **2009**, *167*, 630–633.
Groundnut-shell-derived activated carbon	165	*Dyes Pigm.* **2001**, *51*, 25–40.
Perlite	162	*Water Air Soil Pollut.* **2000**, *120*, 229–248.
Hair	158	*Water Air Soil Pollut.* **1999**, *114*, 423–438.
Diatomite (Jordan)	157	*Appl. Clay Sci.* **2003**, *24*, 111–120.

Graphene	154	*Colloids Surf. B* **2012**, *90*, 197–203.
Cobalt doping hectorite	151	*J. Hazard. Mater.* **2010**, *175*, 965–969.
Bamboo dust activated carbon	143	*Dyes Pigm.* **2001**, *51*, 25–40.
Bagasse bottom ash	143	*Res. J. Chem. Environ.* **2002**, *6*, 61–65.
Hair	120	*Water Air Soil Pollut.* **1986**, *29*, 273–283.
Sewage sludge from an urban wastewater	115	*Biochem. Eng. J.* **2003**, *15*, 59–68.
Crushed brick	97	*J. Hazard. Mater.* **2006**, *135*, 264–273.
Tea waste	85	*J. Hazard. Mater.* **2009**, *164*, 53–60.
Al-MCM-41	78	*J. Hazard. Mater.* **2010**, *178*, 349–355.
Fly ash	54	*J. Am. Inst. Chem. Eng.* **1974**, *20*, 228–238.
Carbonised press mud	50	*Res. J. Chem. Environ.* **2002**, *6*, 61–65.
Magnetite-loaded MWCNTs	48	*J. Hazard. Mater.* **2011**, *198*, 282–290.
Biopolymer oak sawdust	38	*J. Am. Sci.* **2010**, *6*, 267–283.
Perlite	31	*Water Air Soil Pollut.* **2000**, *120*, 229–248.
Banana Peel	21	*J. Hazard. Mater.* **2002**, *92*, 263–275.
Orange Peel	19	*J. Hazard. Mater.* **2002**, *92*, 263–275.
Natural tripoli	17	*Am. J. Environ. Sci.* **2009**, *5*, 197–208.
Sunflower seed	16	*Bioresour. Technol.* **2008**, *14*, 6214–6222.
Hazelnut-shell-derived activated carbon	8.8	*Micropor. Mesopor. Mater.* **2003**, *66*,189–95.

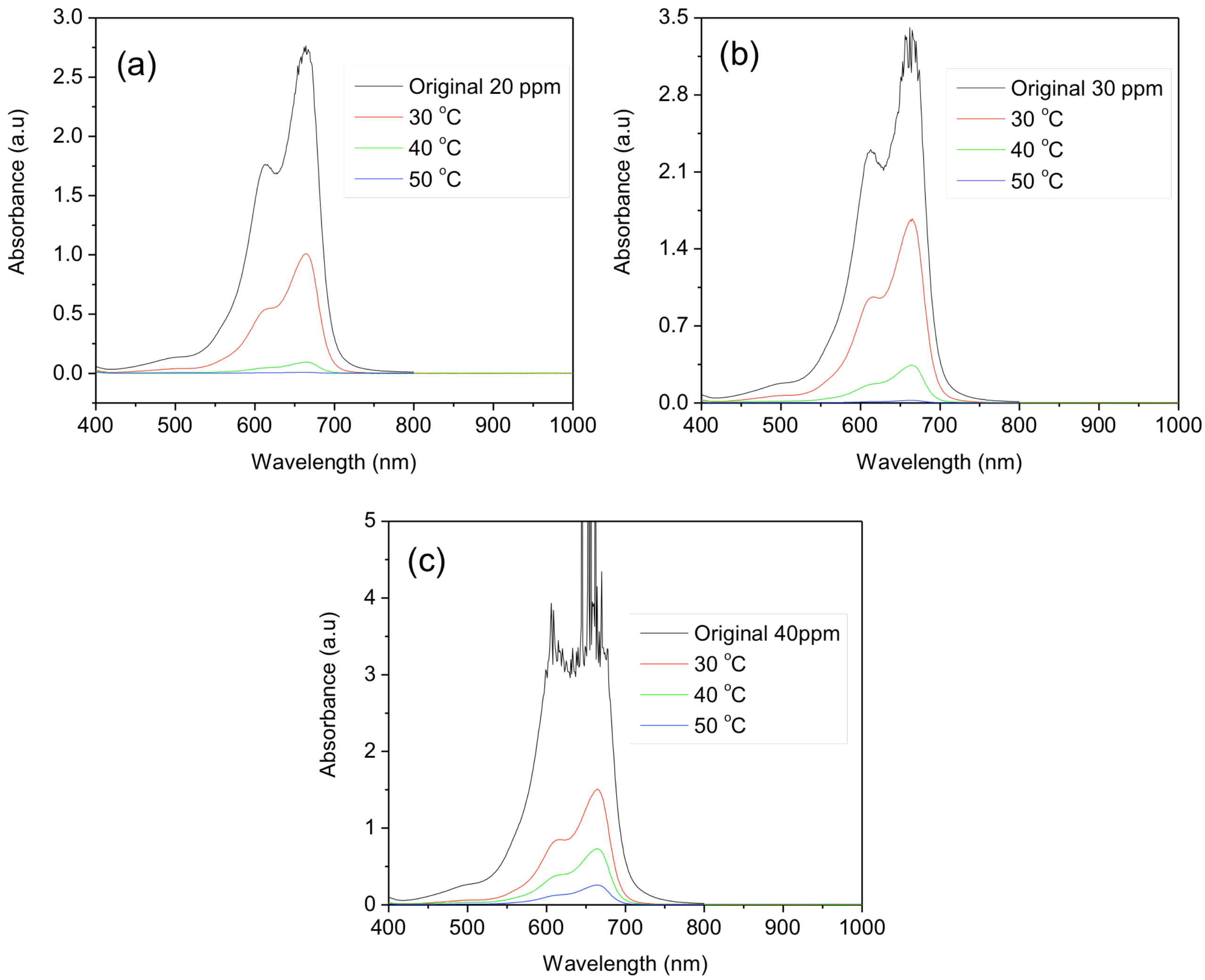

Fig. S9. Comparison of UV-visible spectra of a MB solution during adsorption over 5 mg amino-MIL-101(Al) at different temperatures. (a) $[MB]_0$ = 20 ppm, (b) $[MB]_0$ =30 ppm, (c) $[MB]_0$ =40 ppm.

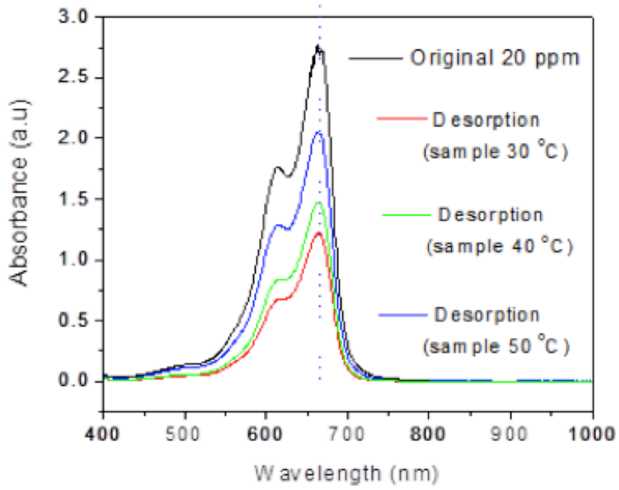

Fig. S10. Comparison of the UV-visible spectrum of MB (20 ppm) with those of dyes desorbed from MOF–MB composites during sonication in water for 12 h. MOF–MB composites were prepared by adsorption of MB ($[MB]_0$ = 20 ppm) on 5 mg of amino-MIL-101(Al) for 12 h, at 30, 40 or 50 °C.

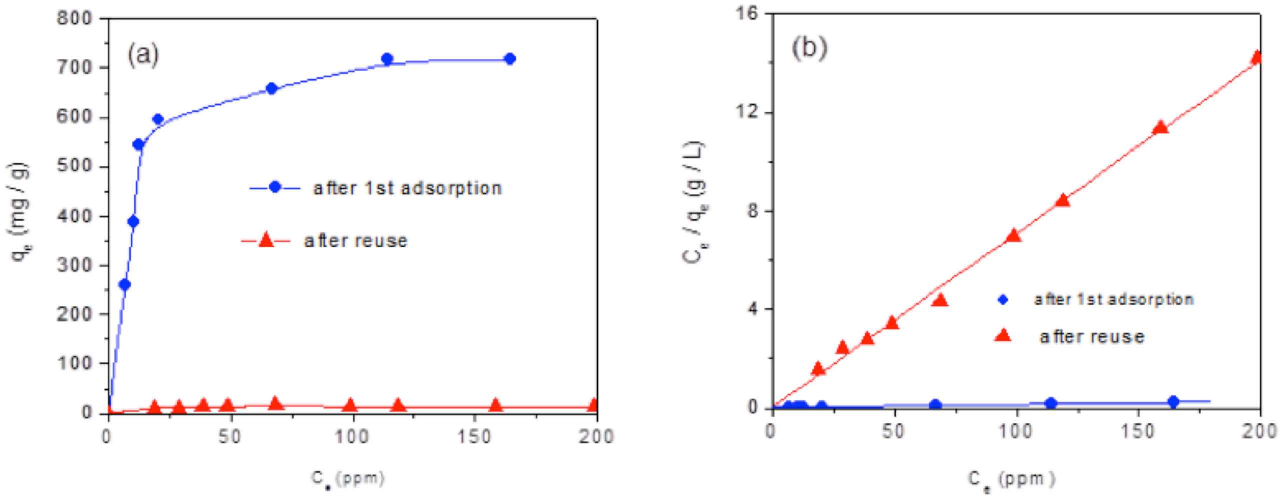

Fig. S11. Reuse of amino-MIL-101(Al) as a sorbent for methylene blue: (a) Isotherms for MB adsorption over fresh (1st adsorption) and used amino-MIL-101(Al) (5 mg) after 12 h at 30 °C; and (b) Langmuir plots of the isotherms of (a).

4. Rate data and treatment

Pseudo-second-order kinetic treatment: The dye adsorption as a function of time was fit to the pseudo-second-order rate equation shown in its derivative and integrated forms in Eqs. S1 and S2, respectively.[1]

$$\frac{dq_t}{dt} = k_2(q_e - q_t)^2 \qquad \text{Eq. S1}$$

$$\frac{t}{q_t} = \frac{1}{k_2 q_e^2} + \frac{1}{q_e}t \qquad \text{Eq. S2}$$

Where q_e is the amount of dye adsorbed (mg g^{-1}) at equilibrium, and q_t the amount adsorbed at time t. When t/q_t is plotted against t, the second-order kinetic constant (k_2) can be calculated as k_2 = slope^2/intercept.

Pseudo-first-order kinetic treatment: The dye adsorption as a function of time over the period t = 5–60 min was fit to the pseudo-first-order rate equation (integrated form shown in Eq. S3).

$$\ln(q_e - q_t) = \ln q_e - k_1 t \qquad \text{Eq. S3}$$

From Equation S3, the kinetic constant (k_1) of a pseudo-first-order reaction is equal to the slope of a plot of $\ln(q_e - q_t)$ vs. t.

Table S2. Pseudo-second-order kinetic 'constants' (k_2) for the adsorptions of MB and MO on amino-MIL-101(Al) at $[\text{dye}]_0$ = 20 or 30 ppm, along with correlation constants (R^2) for the plots of t/q_t vs. t used to derive the values.

Dye	Pseudo-second-order kinetics constants k_2 (g mg^{-1} min^{-1})[a]			
	20 ppm		30 ppm	
	k_2	R^2	k_2	R^2
MB	8.61×10^{-4}	0.996	1.06×10^{-3}	0.997
MO	6.23×10^{-5}	0.992	8.30×10^{-5}	0.973

[a]The data were not completely described by either first- or second-order models, so the rate 'constants' depend on $[\text{dye}]_0$. Values are derived from data in Figures S8a and S14a. See Table 1 for $[\text{dye}]_0$ = 40 ppm.

Table S3. Pseudo-first-order kinetic 'constants' (k_1) for the adsorptions of MB and MO on amino-MIL-101(Al) at $[\text{dye}]_0$ = 20 or 30 ppm, along with correlation constants (R^2) for the plots of $\ln(q_e - q_t)$ vs. t used to derive the values.

Dye	Pseudo-first-order kinetics constants k_1 (min^{-1})[a]			
	20 ppm		30 ppm	
	k_1	R^2	k_1	R^2
MB	0.0432	0.992	0.0584	0.989
MO	0.00369	0.995	0.00540	0.972

[a]The data were not completely described by either first- or second-order models, so the rate 'constants' depend on $[\text{dye}]_0$. Values are derived from data in Figures S8b and S14b. See Table 1 for $[\text{dye}]_0$ = 40 ppm.

Electronic Supplementary Material (ESI) for Journal of Materials Chemistry A

5. XPS analysis of amino-MIL-101(Al) before and after MB adsorption

X-ray photoelectron spectroscopy (XPS, ESCALAB250Xi, Thermo scientific, UK; X-ray source: monochromated Al Kα, Power: 164 W (10.8 mA and 15.2 kV); binding energy reference: C1*s* = 285.0 eV for adventitious hydrocarbon) was used to examine the chemical states of different elements in amino-MIL-101(Al) before and after MB adsorption (Figure S12). The XPS results are detailed in Tables S4 and S5.

Table S4. XPS data for amino-MIL-101(Al).

Orbital	$E_{binding}$, start (eV)	$E_{binding}$, peak (eV)	$E_{binding}$, end (eV)	FWHM[a] (eV)	Peak Area (Counts eV s^{-1})	Atom % (%)	Coefficient[b]
C1*s* A	294.38	284.92	281.48	1.49	28829.48	29.22	1
C1*s* B	294.38	286.44	281.48	1.49	8209.94	8.32	1
C1*s* C	294.38	289.09	281.48	1.49	12156.84	13.49	1
C1*s* D	294.38	290.7	281.48	1.49	1756.91	1.78	1
Al2*p*	78.98	75.06	72.38	1.59	4008.36	7.46	0.537
N1*s* A	403.88	399.61	395.28	1.61	9090.85	5.18	1.8
N1*s* B	403.88	401.39	395.28	1.61	2593.65	1.48	1.8
O1*s*	537.08	532.41	527.68	1.92	92826.29	33.07	2.93

[a] Full width at half maximum. [b] Atom-specific coefficient used to calculate sample composition.

Table S5. XPS data for amino-MIL-101(Al) following adsorption of MB ($[MB]_0$ = 40 ppm, T = 30 °C, t = 12 h).

Orbital	$E_{binding}$, start (eV)	$E_{binding}$, peak (eV)	$E_{binding}$, end (eV)	FWHM[a] (eV)	Peak Area (Counts eV s^{-1})	Atom % (%)	Coefficient[b]
C1s A	293.58	284.97	281.98	1.43	23786.21	29.60	1
C1s B	293.58	286.25	281.98	1.43	13780.05	16.11	1
C1s C	293.58	287.77	281.98	1.43	2822.95	2.41	1
C1s D	293.58	289.08	281.98	1.43	6592.63	8.21	1
C1s E	293.58	290.74	281.98	1.43	1127.74	1.40	1
Al2p	78.98	74.86	71.88	1.64	2278.7	7.34	0.537
N1s	404.08	399.71	395.98	1.8	9960.15	6.97	1.8
O1s	537.38	532.25	527.68	2.01	60436.62	26.43	2.93
S2p3 A	171.68	164.65	161.52	1.41	1121	1.25	1.11
S2p3 B	171.68	168.05	161.52	1.77	168.84	0.18	1.11
F1s A	694.88	689.48	684.88	1.75	353.18	0.10	4.43

[a] Full width at half maximum. [b] Atom-specific coefficient used to calculate sample composition.

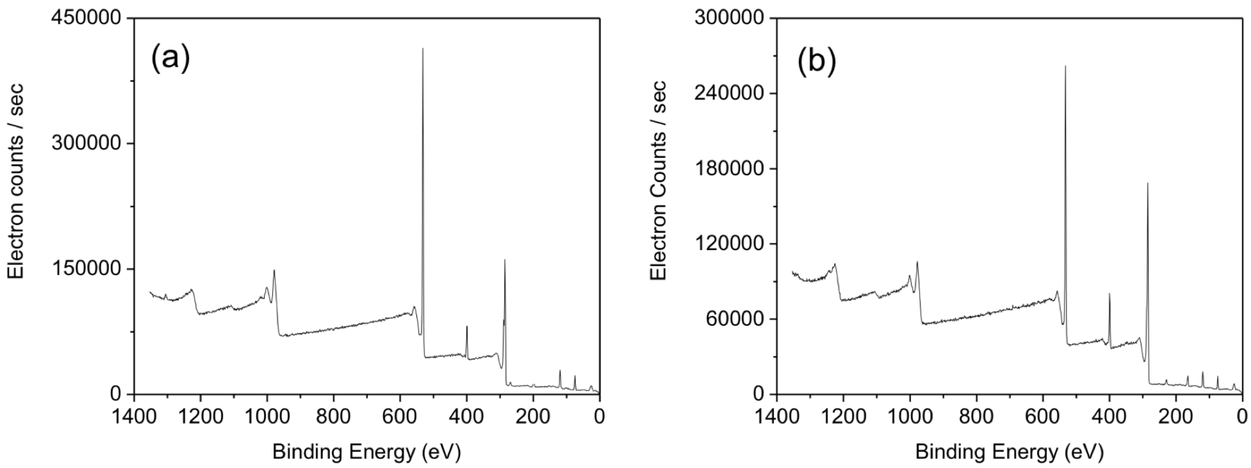

Fig. S12. XPS of amino-MIL-101(Al) (a) as-prepared; (b) after adsorption of MB for 12 h at 30 °C ($[MB]_0$ = 40 ppm).

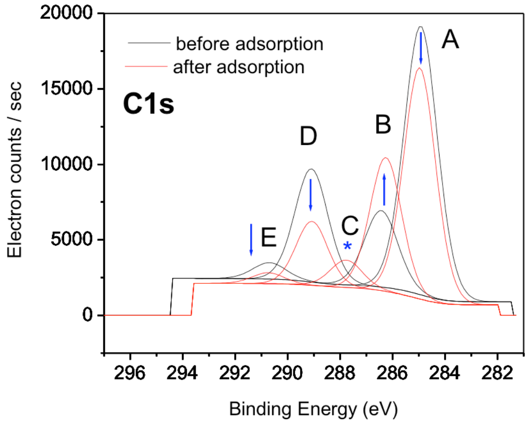

Fig. S13. C1*s* region of the XPS patterns of amino-MIL-101(Al) after and before adsorption of MB for 12 h at 30 °C ($[MB]_0$ = 40 ppm).

6. Adsorption of methyl orange (MO)

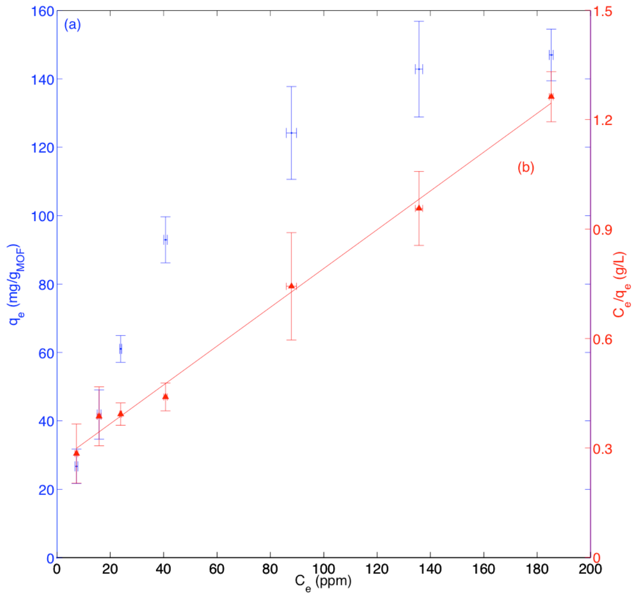

Figure S14. (a) Isotherm for MO adsorption over 5 mg of amino-MIL-101(Al) after 12 h at 30 °C; (b) Langmuir plot of the isotherm in (a), straight line is $C_e/q_e = 0.00532\ C_e + 0.260$.

Table S6. Maximum adsorption capacity of methyl orange (MO) on various adsorbents.

Adsorbent	Maximum Adsorption Capacity, Q_o (mg g^{-1})	Reference
Biomass (*Schinopsis balansae*)	483	*J. Hazard. Mater.* **2010**, *174*, 9–16.
MOF-235	477	*J. Hazard. Mater.* **2011**, *185*, 507–511.
Coal-based activated carbon from anthracite	448	*Ind. Eng. Chem. Res.* **1991**, *30*, 2411–2416.
Coconut-husk-based activated carbon	435	*J. Hazard. Mater.* **2008**, *154*, 337–346.
Sunflower stalks	428	*Color. Technol.* **2004**, *118*, 256–269.
Coconut-shell-derived activated carbon	368	*Ind. Eng. Chem. Res.* **1991**, *30*, 2411–2416.
Secondary bagasse pith	339	*Color. Technol.* **2002**, *118*, 256–269.
Clay	300	*Ann. Chim. Sci. Mater.* **2000**, *25*, 615–626.
Rattan-sawdust-derived activated carbon	294	*Dyes Pigm.* **2007**, *75*, 143–149.
Cotton waste	277	*Water Air Soil Pollut.* **1999**, *114*, 423–438.

Activated sludge biomass	256	*J. Hazard. Mater. B* **2004**, *108*, 183–188.
Cotton waste	240	*Color. Technol.* **2005**, *118*, 256–269.
Jute fiber Carbon	226	*J. Colloid Interface Sci.* **2005**, *284*, 78–82.
MIL-101(Cr)	194	*J. Hazard. Mater.* **2010**, *181*, 535–542.
Amino-MIL-101(Al)	**188 ± 9**	**This work**
Diatomite	157	*J. Environ. Manage.* **2003**, *69*, 229–238.
Spirodela polyrrhiza biomass	145	*Environ. Pollut.* **2003**, *125*, 385–392.
Coir pith	120	*Waste Manage.* **2001**, *21*, 381–387.
Tea waste	85	*J. Hazard. Mater.* **2009**, *164*, 53–60.
Raw date pits	80	*Process Biochem.* **2003**, *39*, 193–202.
Fly ash	76	*Water Res.* **2003**, *37*, 4938–4944.
Peanut hull	68	*J. Hazard. Mater.* **2005**, *121*, 247–250.
MCM-22	1.8×10^{-4} mol/g	*J. Colloid Interface Sci.* **2006**, *295*, 71–78.
Rice husk	41	*J. Colloid Interface Sci.* **2005**, *286*, 90–100.
Fe(III)/Cr(III) hydroxide	23	*J. Environ. Manage.* **2005**, *74*, 207–215.
Banana peel	21	*J. Hazard. Mater.* **2002**, *92*, 263–274.
Orange peel	21	*J. Hazard. Mater.* **2002**, *92*, 263–274.
Dead fungus *Aspergillus niger*	19	*Water Qual. Res. J. Can.* **2000**, *35*, 95–111.
Silica	11	*Appl. Geochem.* **2002**, *17*, 1159–1164.
Neem leaf powder	8.8	*Dyes Pigm.* **2005**, *65*, 51–59.
Clay	6.3	*J. Colloid Interf. Sci.* **2004**, *269*, 310–314.
Fly ash	5.6	*J. Colloid Interface Sci.* **2005**, *284*, 14–21.
Glass fibers	2.2	*J. Colloid Interface Sci.* **2005**, *286*, 807–811.

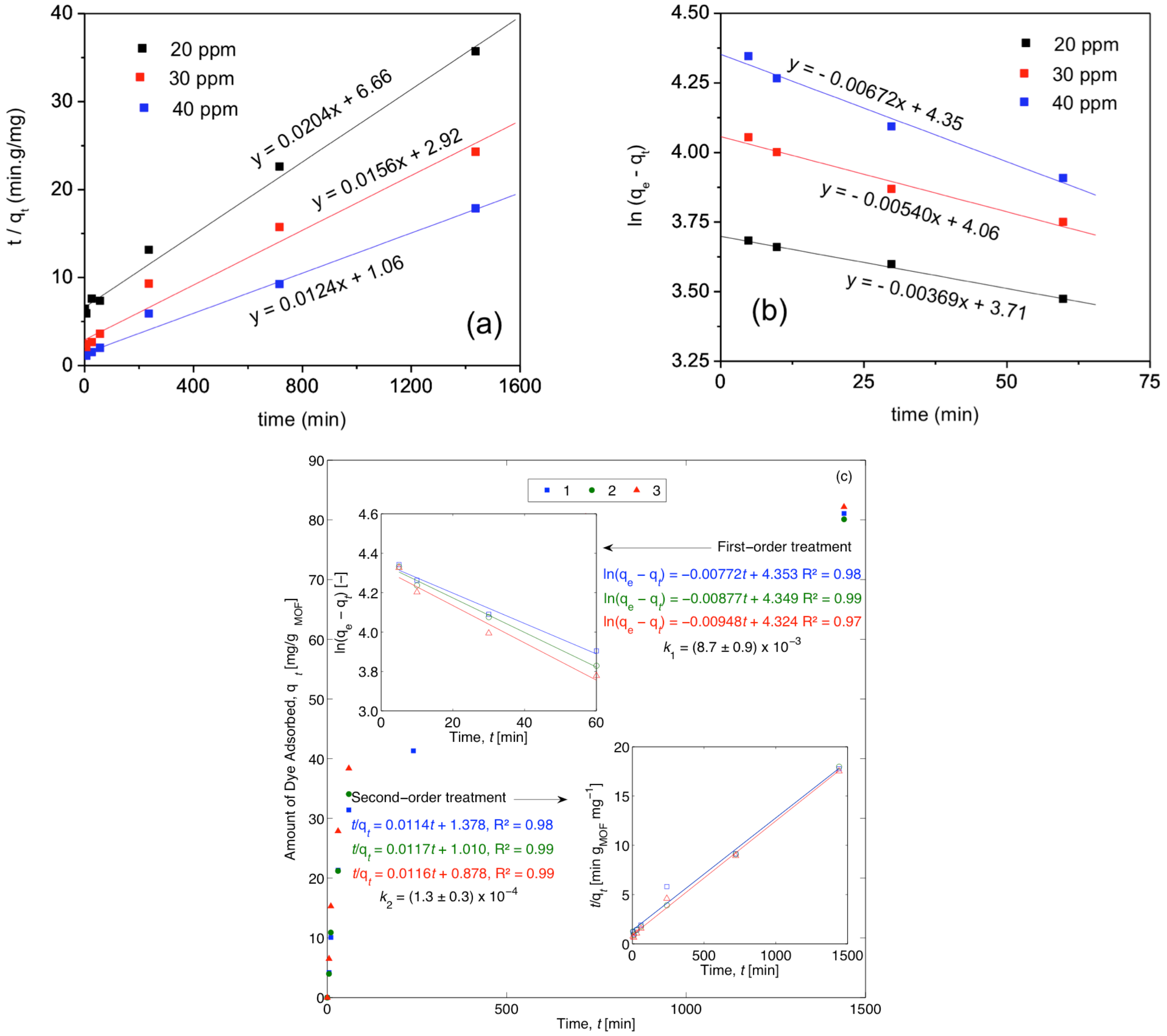

Fig. S15. Plots of (a) pseudo-second-order and (b) pseudo-first-order kinetics for MO adsorption over 5 mg amino-MIL-101(Al) at 30 °C and $[MB]_0$ = 20, 30 or 40 ppm. (c) Three replicates of the adsorption of MO over 5 mg amino-MIL-101(Al) at 30 °C and $[MB]_0$ = 40 ppm, with accompanying kinetic fits.

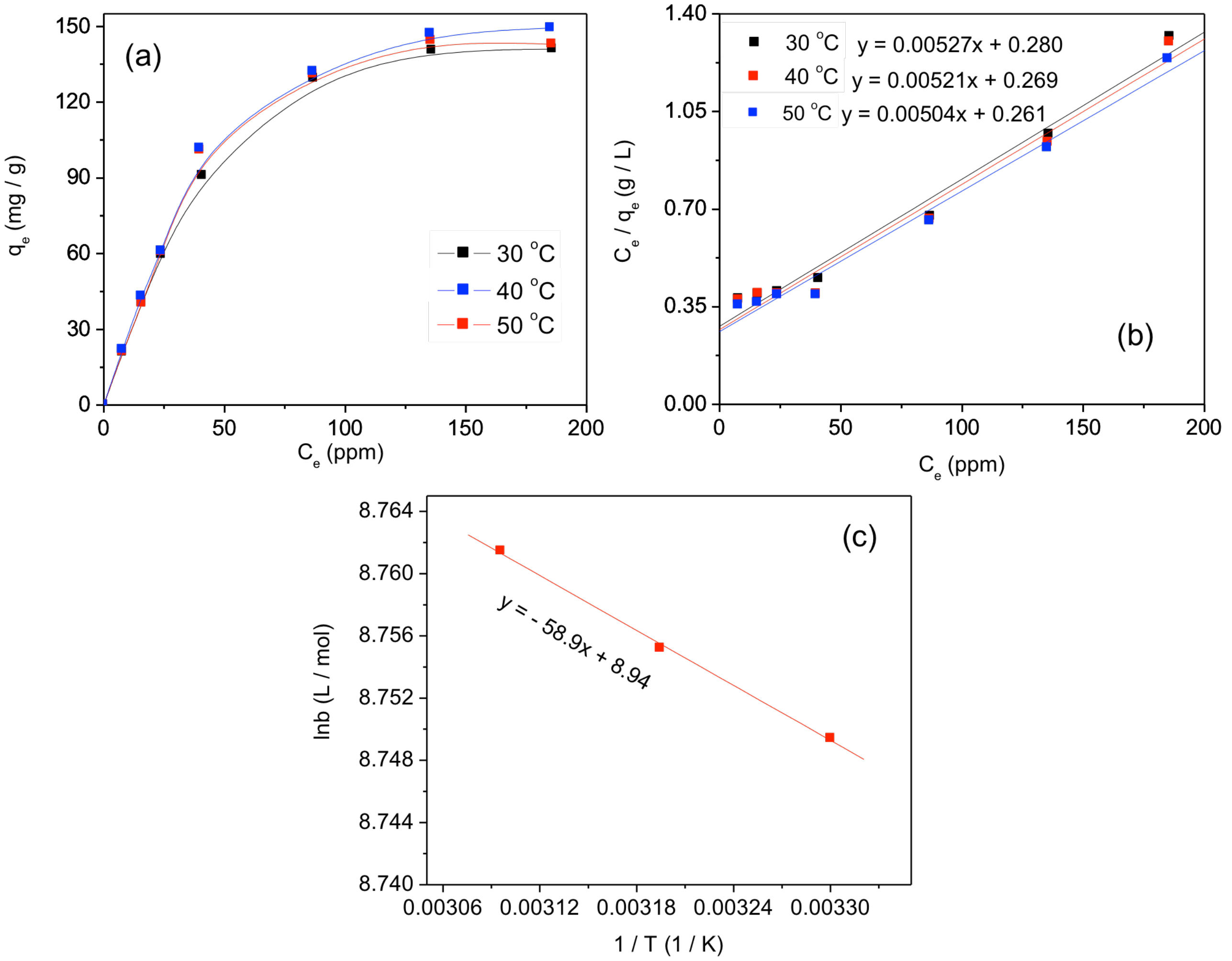

Fig. S16. (a) Isotherms for MO adsorption over 5 mg of amino-MIL-101(Al) for 12 h at 30, 40 and 50 °C; (b) Langmuir plots of the isotherms in (a); (c) van't Hoff plot of the Langmuir constants b as a function of temperature, used to calculate the ΔH and ΔS of the MO adsorption over amino-MIL-101(Al).

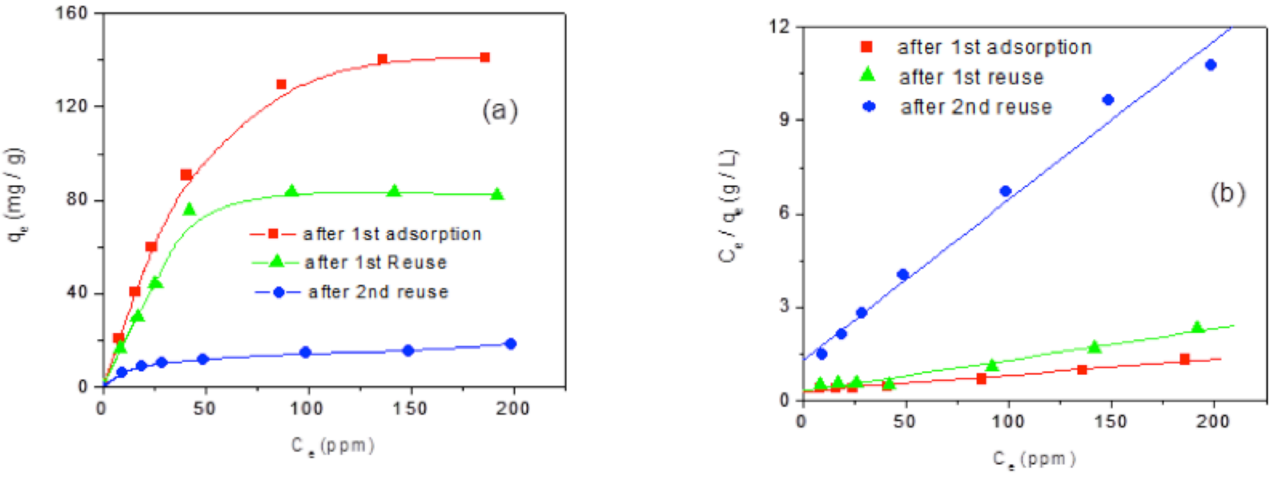

Fig. S17. Reuse of amino-MIL-101(Al) as a sorbent for methyl orange. (a) Isotherms for MO adsorption over fresh (1st adsorption) and used amino-MIL-101(Al) (5 mg) after 12 h at 30 °C; and (b) Langmuir plots of the isotherms of (a).

7. Comparison of MB and MO adsorption on amino-MIL-101(Al)

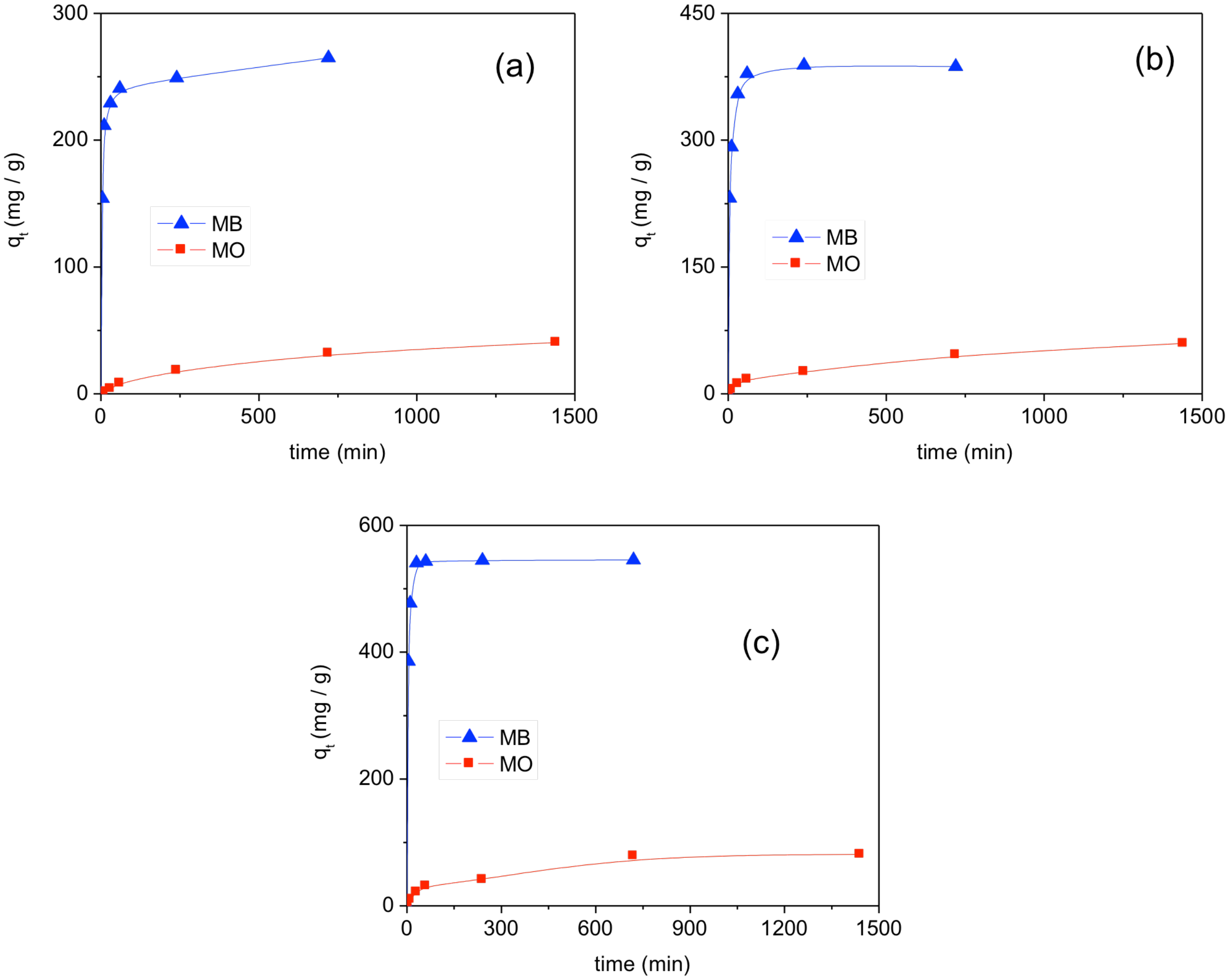

Fig. S18. Comparison between the rates of MB and MO adsorption over 5 mg of amino-MIL-101(Al) at 30 °C at $[dye]_0$ = (a) 20 ppm; (b) 30 ppm; and (c) 40 ppm.

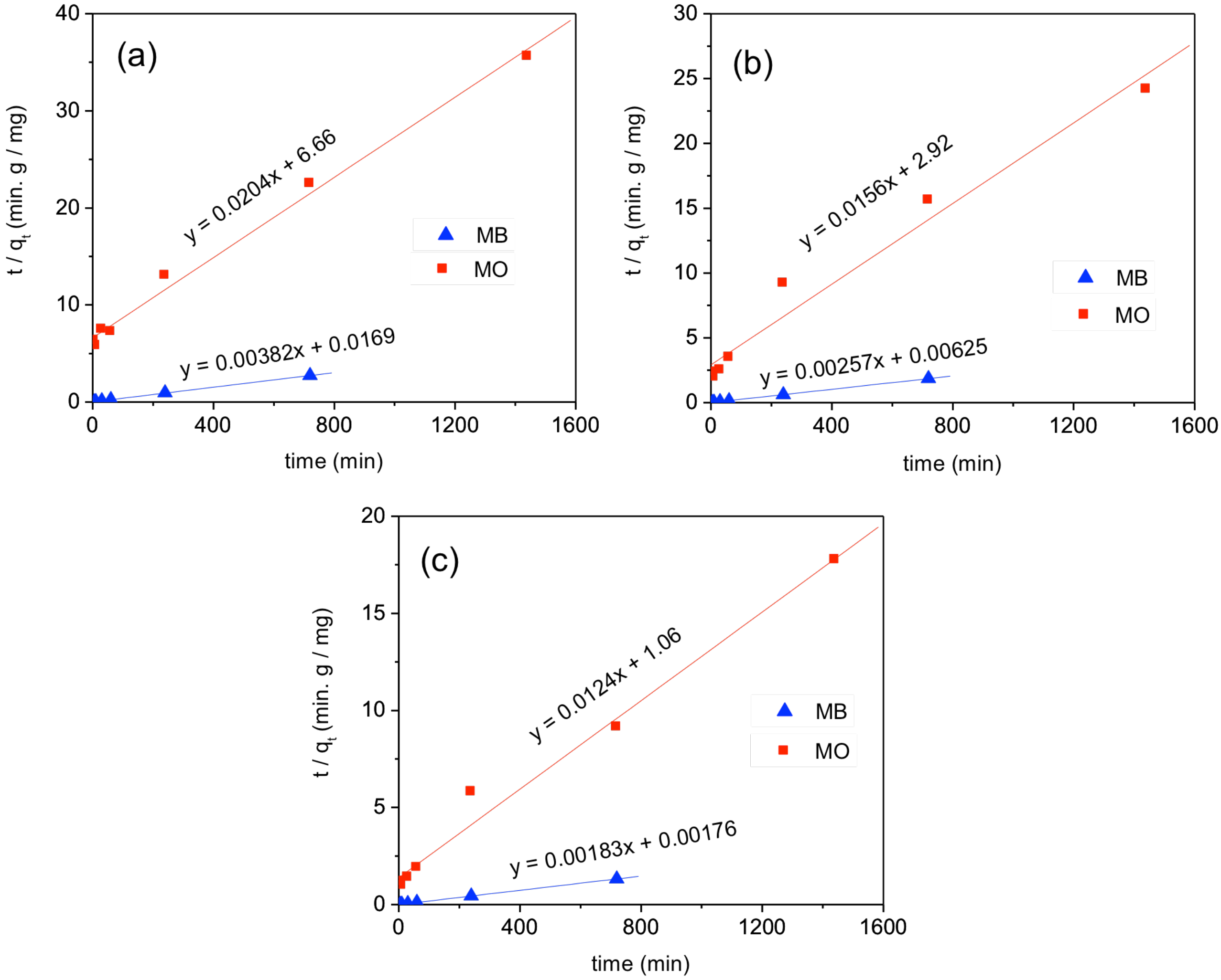

Fig. S19. Pseudo-second-order kinetic treatment of MB and MO adsorption over 5 mg of amino-MIL-101(Al) at 30 °C and $[dye]_0$ = (a) 20 ppm; (b) 30 ppm; and (c) 40 ppm.

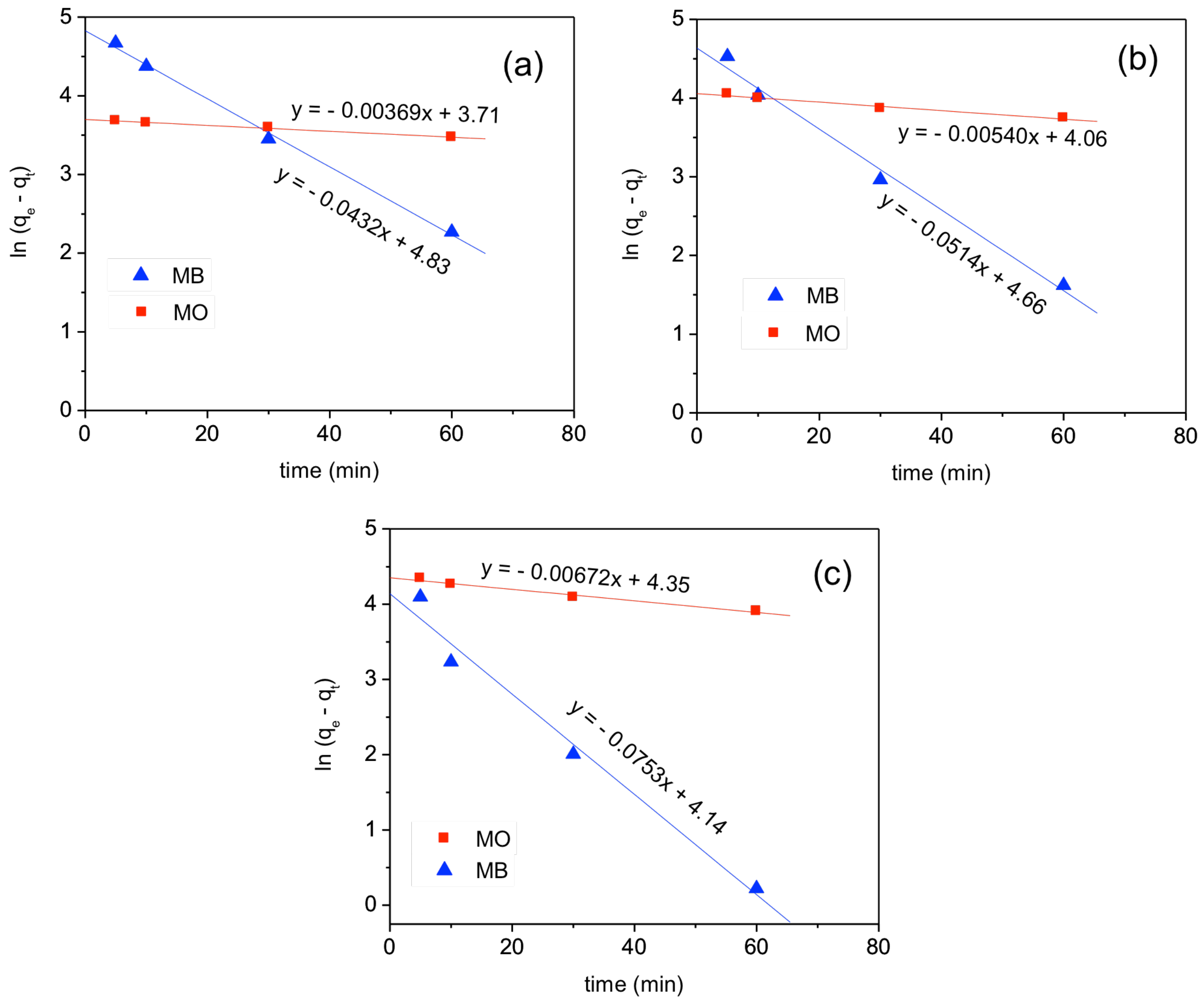

Fig. S20. Pseudo-first-order kinetic treatment of MB and MO adsorption over 5 mg of amino-MIL-101(Al) at 30 °C and $[dye]_0$ = (a) 20 ppm; (b) 30 ppm; and (c) 40 ppm.

8. Characterisation of amino-MIL-101(Al) after dye exposure

Samples of amino-MIL-101(Al) were exposed to MB or MO ([dye]$_0$ = 40 ppm) for 12 h at 50 °C, then separated from the solution by filtration and analysed using N_2 physisorption and ^{27}Al NMR. The results are shown in Figures S21 and S22, respectively.

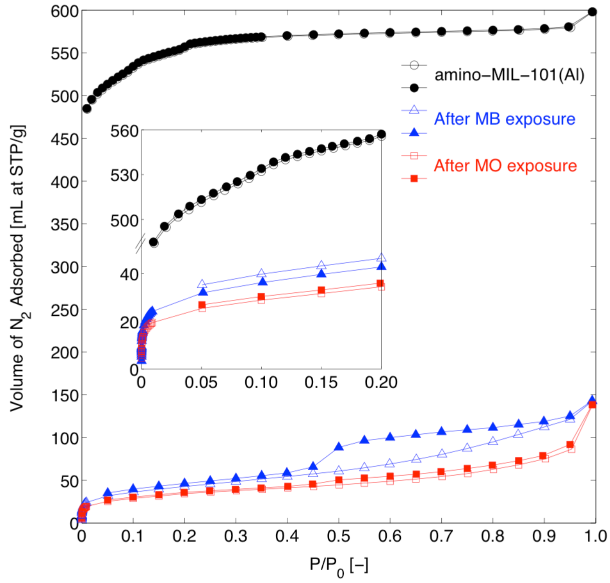

Fig. S21. N_2 adsorption–desorption isotherms of amino-MIL-101(Al) before adsorption, after MB adsorption, and after MO adsorption. Isotherms were acquired at −196 °C. Dye adsorptions used [dye]$_0$ = 40 ppm, T = 50 °C, and t = 12 h.

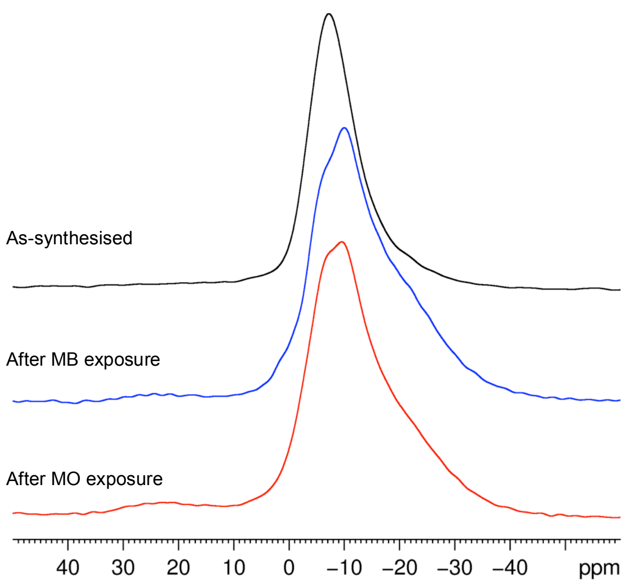

Fig. S22. Magic-angle spinning (MAS) ^{27}Al NMR spectra of amino-MIL-101(Al) before adsorption, after MB adsorption, and after MO adsorption. Recorded at 182.49 MHz, spinning at the magic angle at 20 kHz at ambient temperature. Data was acquired using a single pulse (~14°, π/12 pulse) with a 1-s recycle delay. Dye adsorptions used [dye]$_0$ = 40 ppm, T = 50 °C, and t = 12 h.

Electronic Supplementary Material (ESI) for Journal of Materials Chemistry A

9. Adsorption of MB on MIL-101(Al)

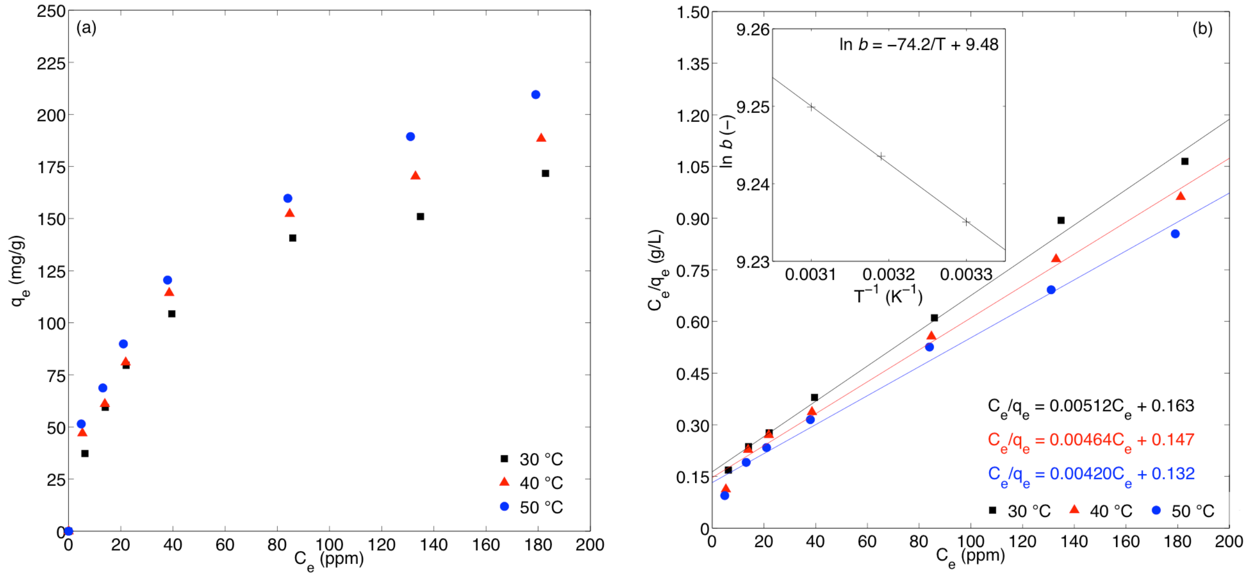

Fig. S23. (a) Isotherms for MB adsorption over 5 mg of MIL-101(Al) for 12 h at 30, 40 and 50 °C; (b) Langmuir plots of the isotherms in (a) and (inset) van't Hoff plot of the Langmuir constants b as a function of temperature.

10. Reference

1. Y. S. Ho and G. McKay, *Process Biochem.*, 1999, **34**, 451-465.